J. Membrane Biol. 181, 55–65 (2001)
DOI: 10.1007/s0023200100073

The Journal of
Membrane
Biology

© Springer-Verlag New York Inc. 2001

Conduction of Monovalent and Divalent Cations in the Slow Vacuolar Channel

I.I. Pottosin, O.R. Dobrovinskaya, J. Muñiz
Centro Universitario de Investigaciones Biomedicas, Av. 25 de Julio s/n, Apdo Postal/P.O. Box #199, 28047 Colima, Mexico

Received: 18 September 2000/Revised: 19 January 2001

Abstract. The conduction properties of individual physiologically important cations Na^+, K^+, Mg^{2+}, and Ca^{2+} were determined in the slowly activating (SV) channel of sugar beet vacuoles. Current-voltage relationships of the open channel were measured on excised tonoplast patches in a continuous manner by applying a ±140 mV ramp-wave protocol. Applying KCl gradients of either direction across the patch we have determined that the relative Cl^- to K^+ permeability was ≤1%. Symmetrical increase of the concentration of tested cation caused an increase of the single channel conductance followed by saturation. Fitting of binding isotherms at zero voltage to the Michaelis-Menten equation resulted in values of maximal conductance of 300, 385, 18, and 13 pS, and of apparent dissociation constants of 64, 103, 0.04, and 0.08 mM for Na^+, K^+, Mg^{2+}, and Ca^{2+}, respectively. Deviations from the single-ion occupancy mechanism are documented, and alternative models of permeation are discussed. The magnitude of currents carried by divalent cations at low concentrations can be explained by an unrealistically wide (~140 Å) radius of the pore entrance. We propose instead a fixed negative charge in the pore vestibules, which concentrates the cations in their proximity. The conduction properties of the SV channel are compared with reported characteristics of voltage-dependent Ca^{2+}-permeable channels, and consequences for a possible reduction of postulated multiplicity of Ca^{2+} pathways across the tonoplast are drawn.

Key words: Calcium and magnesium conduction — Potassium and sodium — Binding and saturation — Slow vacuolar channel — Patch-clamp — Vacuole

Introduction

The slowly activating (SV) channel is the ubiquitous component of the vacuolar membrane of higher plants (Hedrich et al., 1988). Because of its abundance, high conductance for monovalent and divalent cations, and activation by cytosolic Ca^{2+} increase, the SV channel was, as a possible Ca^{2+} release channel, in the focus of numerous studies carried out in the last years (Ward and Schroeder, 1994; Schulz-Lessdorf & Hedrich, 1995; Allen & Sanders, 1996; Pottosin et al., 1997; Pei, Ward & Schroeder, 1999). Our quantitative study (Pottosin et al., 1997) on the regulation of the SV channel by cytosolic and vacuolar Ca^{2+} and by membrane voltage yielded very low activity (less than one open SV channel per vacuole) at physiologically attainable electrochemical gradients for Ca^{2+}, thus apparently leaving little room for a postulated role of the SV channel in Ca^{2+}-induced Ca^{2+} release (Ward & Schroeder, 1994; for discussion see MacRobbie, 1998; White, 2000). This possibility could be reconsidered, however, in the light of the recent report on the potentiation of the stimulatory Ca^{2+} effect by cytosolic Mg^{2+} (Pei et al., 1999).

Another issue to be resolved, before considering a meaningful physiological function of the SV channel, was its selective permeability. Our previous study on the block of the SV channel by permeant organic cations defined a large (~7 Å) diameter of the pore in the narrowest cross-section (Dobrovinskaya, Muñiz & Pottosin, 1999), so there are no mechanistic barriers for the conduction of most of the inorganic ions. Apparently, the ions are selected not by sieving but on the basis of their electrostatic interaction with the pore walls. Despite earlier confusion (Hedrich & Kurkdjian, 1988; Schulz-Lessdorf & Hedrich, 1995) it seems to be widely accepted now that the anion permeability of the SV channel is low if there is any at all. However, the precision of the results obtained so far cannot exclude some Cl^- permeability up to 10% of that for K^+. It is known, that the SV channel has about 10 times lower conductance although a somewhat higher relative permeability for divalent cations, Ba^{2+} and Ca^{2+}, compared to K^+ (Pantoja, Gelli & Blumwald, 1992*b;* Ward & Schroeder, 1994). The SV channel weakly selects between alkali cations, particu-

Correspondence to: I.I. Pottosin

larly between K^+ and Na^+, and has a comparable conductance for these ions at 200 mM concentration (Amodeo, Escobar & Zeiger, 1994). Recently, a kinetic study of the mechanism of Ca^{2+}/K^+ selectivity in the SV channel appeared (Allen, Sanders & Gradmann, 1998). This work offered a number of testable predictions on the binding and voltage-dependent conduction of Ca^{2+} and K^+, which came well beyond the range of voltages and ion concentrations documented there. We are not aware of any experimental attempt to define the conductance-activity relation for Ca^{2+} in the SV channel. Test of this relation for K^+ resulted in contradictory conclusions on the existence of binding site(s) within the pore, saturated at concentrations of K^+ in the physiological range (Schulz-Lessdorf & Hedrich, 1995; Gambale et al., 1996). A macroscopic SV current, carried by Mg^{2+}, was detected (Pottosin et al., 1997), but nothing is known about Mg^{2+} conduction at the single channel level.

The present study was designed, therefore, to measure the individual conductance-activity relations for the physiologically important ions Na^+, K^+, Mg^{2+}, and Ca^{2+} in the SV channel. We used the advantage of slow kinetics of the channel to obtain the open channel current-voltage relationships in continuous manner, as the channel could be stochastically locked in the closed or in the open state during short ramp-wave changes of the clamped voltage. This technique, besides accumulation of large statistics in a relatively short time, also allowed us to expand the range of experimental voltages compared to previous studies of other authors. A nonlinear shape of current-voltage relationships of the SV channel was revealed with a precision that served as a good basis for testing the theoretical models. A complete set of current-voltage relationships for divalent cations in the 0.2–30 mM range and for monovalent cations in the 5–500 mM range was obtained. On the basis of its comparison with results of other authors, the relation between voltage-dependent Ca^{2+}-conducting currents of the vacuolar membrane was rationalized.

Materials and Methods

Isolation of Vacuoles, Patch-Clamp Media and Recording

Fresh *Beta vulgaris* (whole plants) were received once a week from a local market and kept at +4°C before use. Prior to isolation of vacuoles, slices of a taproot were incubated 0.5–1 hr at +25°C in a solution equivalent to the bath solution used in experiments. The osmolality of solutions was adjusted with sorbitol to isotonic or slightly hypertonic with respect to the vacuolar sap as verified by a cryoscopic osmometer (OSMOMAT 030, Gonotec, Germany). The osmolality of the vacuolar sap was subjected to seasonal changes being 550–700 mOs in winter months, but dropping to 400–550 before and during the rain period. For isolation of vacuoles a single tissue slice (~300 mg weight) was transferred to a Petri dish containing 3–3.5 ml of fresh solution, and cut by preparative needles. Few (1–5) released vacuoles were collected by a micropipette (5–10 μl volume) and transferred to the experimental chamber (300 μl volume). After adhesion of vacuoles to the bottom, ~10 volumes of fresh solution were passed through the chamber to remove the contamination. All experiments were carried out at room temperature (23–25°C). The pH of all experimental solutions was adjusted to 7.5 with HEPES titrated by NaOH or KOH in case of monovalent cation series, and by $Ca(OH)_2$ in case of divalent cation series. The solutions for the range of concentrations of K^+ and Na^+ 30–500 mM contained (besides KCl or NaCl) 15 mM HEPES and 2 mM nitrilotriacetic acid (NTA). In 10 mM solutions HEPES was reduced to 10 mM, and in 5 mM ones, HEPES and NTA were reduced to 0.5 mM. $CaCl_2$ was added to give a final free Ca^{2+} concentration (activity) of 50 μM as calculated using Winmaxc v1.78 software with the constants in BERS.CCM (*see* http://www.stanford.edu/~cpatton/maxc.html); the calculation was corrected for the ionic strength of solutions. For Ca^{2+} series in the range of concentrations 1 to 30 mM, the solutions, besides $CaCl_2$, contained 0.5 mM $Ca(OH)_2$ + 2 mM HEPES, solutions of 0.2 and 0.5 mM Ca^{2+} were prepared by dilution of the 1 mM Ca^{2+} solution with isotonic sorbitol solution. For Mg^{2+} series in the range of concentrations 1 to 30 mM the solutions, besides $MgCl_2$, contained 0.1 mM $Ca(OH)_2$ + 0.5 mM HEPES; solutions of 0.2 and 0.5 mM Mg^{2+} were prepared by dilution of the 1 mM Mg^{2+} solution. The patch pipette filling solution, except in the experiment presented in Fig. 1, was the same as the bath solution, so no liquid junction potential (LJP) compensation was required. In the case of the experiment of Fig. 1 the LJP was (positive at higher concentration side) 1.0 and 2.1 mV for 500/50 mM and 500/5 mM KCl gradients, respectively, as calculated according to Barry and Lynch (1991). Solutions were prepared on the fresh tridistilled and de-ionized water (ρ = 8–12 MΩ cm). All chemicals were analytical grade (Sigma, St Louis, MO).

Patch pipettes were pulled from Kimax-51 capillaries (Kimble, Toledo, Ohio) in three steps on a Brown/Flaming model P-97 puller (Sutter Instruments Co, Novato, CA), fire polished (LPZ 101 microforge, List Medical, Germany), and covered by Sylgard-curing agent (Dow Corning, Midland, MI). The resistance of patch electrodes filled with a standard 100 mM KCl solution was 3–5 MΩ, 0.7–1 MΩ when filled with 500 mM KCl, and up to 0.5–1.0 GΩ when filled with 0.2 mM Ca^{2+} or Mg^{2+} solutions. Current measurements were performed using an Axopatch 200A Integrating Patch-Clamp amplifier (Axon Instruments, Foster City, CA). The measurements of vacuolar ion currents were done under voltage-clamp conditions using outside-out (cytoplasmic side of the membrane faces the bath) or inside-out patches (Hamill et al., 1981). To register single-channel currents carried by divalent cations in a broad voltage range we mainly utilized inside-out (vacuolar-side-out) patches, obtained by brief air-exposure of the patch-pipette after the achievement of initial GΩ-seal contact with the vacuolar membrane. To insure the correct orientation of the membrane before detachment of the pipette, the currents in the vacuole-attached configuration were inspected, although usually not recorded. Unitary currents in the vacuole-attached mode generally have larger amplitudes than in excised patches, due to a higher salt concentration inside the vacuole, but displayed the same asymmetric behavior, i.e., activation by pipette (cytosol) positive voltages and rapid deactivation at negative ones. To obtain the outside-out (cytosolic-side-out) configuration we usually utilized a short high-voltage pulse to break down the patch membrane. This operation was routinely performed in the low-Ca^{2+} medium used for the monovalent cation series. In the presence of high concentrations of divalent cations at both membrane sides, however, high voltage pulses induced persistent instabilities of the patch membrane. The current flowing through these defects interfered with low-amplitude single-channel currents of the SV channels, handicapping their precise registration. However, in some cases the whole-vacuole configuration

was formed spontaneously or by application of a light suction pulse, so the SV currents carried by divalent cations were registered also in the cytosolic-side-out configuration. Because we did not observe any significant difference between properties of currents registered in either configuration, after application of the unified current and voltage convention (*see* below), these data have been included in the overall statistics. The identity of the single-channel currents under investigation with SV channels was routinely confirmed by inspecting slow activation kinetics of the channels in response to positive voltage steps.

The reference AgCl electrode was connected to the bath via a 3% agar bridge filled with 100 mM KCl. The convention of current and voltage was as follows: the sign of voltage refers to the cytosolic side, and positive (outward) currents represent an efflux of cations into the vacuole. The records were filtered at 10 kHz by a low-pass Bessel filter and digitized using a DigiData 1200 Interface (Axon Instruments, Foster City, CA). The single-channel currents were further filtered at 2–5 kHz and recorded directly on a hard disk of an IBM-compatible PC. The command voltage protocols were applied and the analyses were carried out using the pClamp 6.0 software package (Axon Instruments, Foster City, CA). Ramp-wave voltage protocols (between +140 and −140 mV; train of 10 ramps separated by 0.03–2 sec intervals), were applied to obtain unitary-current voltage relationships. The holding potential was selected to ensure that only few SV channels are open. Depending on the SV channel activity, the level of holding potential varied between −40 mV and +140 mV for the monovalent cation series, +80 to +160 mV for the Mg^{2+} series, and +140 to +200 mV for the Ca^{2+} series, increasing with decreasing salt concentration. The duration of a single ramp was normally 30 ms, except in experiments with low divalent concentrations, when the ramp duration, because of faster channel closure, was decreased to 15 ms and the filtering cut-off frequency was increased from 2 kHz to 5 kHz. The successful ramp recordings were sorted for containing 0, 1 or 2 open SV channels, and those not containing any open-channel currents were averaged and subtracted from the latter to obtain a unitary-channel current-voltage characteristic. Segments containing channel closures were erased. To increase the signal-to-noise ratio many individual ramps were averaged.

Data Analysis

Relative permeability of Cl^- to K^+ (*see* Fig. 1) was calculated from the values of zero current potentials, corrected for LJP, using conventional Goldmann-Hodgkin-Katz equation (*see* Hille, 1992). To define the single channel chord conductance the current-voltage relationships were fitted by 4th order polynomials and the coefficient of the 1st term was taken as the value of conductance at zero voltage. For binding isotherms (*see* Figs. 3 & 6) the concentrations were corrected for activity coefficients calculated using a standard Debye-Hückel formalism (Ammann, 1986). To describe the binding isotherm for the chord conductance or for the single-channel current first the Michaelis-Menten equation was used:

$$g(\text{or } i) = \frac{g(\text{or } i)_{max}}{1 + K_m/a} \quad (1)$$

where g (or i)$_{max}$ is the saturated single-channel conductance (or current), a is ionic activity, and K_m is the activity at which the conductance (or current) is 50% of maximal. Alternatively, the conductance (or current)-activity relations were described by the Hill equation:

$$g(0) = \frac{g(0)_{max}}{1 + (K_m/a)^n} \quad (2)$$

where n is the Hill coefficient, defining the order of binding reaction.

Results

Cation Selectivity of the SV Channel

The conventional way for the evaluation of the cation-to-anion selectivity of a channel is to apply a gradient of salt (e.g., KCl) in either direction across the membrane, and to measure the zero-current (reversal) potential of the channel-mediated current. A specific problem with the SV channel is the requirement of high cytosolic Ca^{2+} for the activation. Because Ca^{2+} efficiently competes with K^+ for the pore, the reversal potential is affected, and tends to deviate from the equilibrium potential of K^+ (Ward & Schroeder, 1994; Allen & Sanders, 1995; Pottosin et al., 1997; Allen et al., 1998). Alternatively, other researchers (Schulz-Lessdorf & Hedrich, 1995) interpreted this deviation as a manifestation of significant anion permeability. The precision of the results obtained to date still allowed some 10% Cl^- relative to K^+ permeability. This might be of importance for the channel involved in solute transport across the tonoplast, especially keeping in mind a poor characterization of alternative anion pathways in the vacuolar membrane. To resolve this issue, we have lowered free Ca^{2+} concentration to 50 μM, compared to millimolar used in previous studies, and analyzed the SV channel current-voltage relationships in 500/5 mM and 500/50 mM KCl transmembrane gradients of either direction (Fig. 1). Recording current-voltage (*I/V*) relationships in a continuous manner and averaging a large number of individual *I/V* curves gave us the opportunity to determine the reversal potential of the single-channel current with a great (SD < 1 mV) precision. Reversal potentials (after correction for LJP, *see* Materials and Methods) in 500/50 mM and 50/500 mM (cytosol/vacuole) gradients were −52 and +52 mV, respectively, compared to the equilibrium potentials for K^+ of −54 mV and +54 mV, calculated from the Nernst equation after correction of ionic concentrations for activity coefficients. According to the Goldmann-Hodgkin-Katz equation this implies a value of relative K^+ to Cl^- permeability, P_{K^+}/P_{Cl^-}, of 96. However, with 500/5 mM and 5/500 mM KCl gradients the reversal potentials, −80 mV and +86 mV, respectively, deviated significantly from the equilibrium potential for K^+ (−110 mV and +110 mV). Formally, this implies a decrease of P_{K^+}/P_{Cl^-} to 33 and 47, respectively. A possible origin of this apparent decrease of selectivity will be discussed later. For the purpose of this study it is important to notice that the Cl^- permeability, if there were any, was negligible.

Monovalent Cation Conductance

We have selected K^+ and Na^+ as the physiologically most abundant cations to characterize the binding site(s),

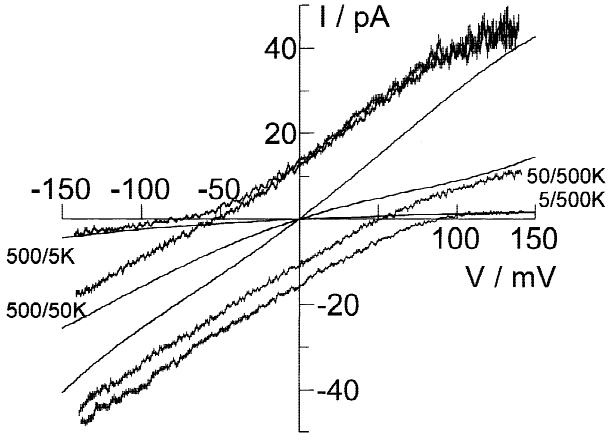

Fig. 1. Current-voltage relationships of the open SV channel in gradients of KCl. The gradient of concentration of KCl (in mM) is indicated for each curve as cytosolic/vacuolar: e.g., 500/5K implies 500 mM KCl at the cytosolic side and 5 mM KCl at the vacuolar side of the tonoplast patch, respectively. The curves are statistical averages (mean ± SD) of 17 (500/5K), 38 (500/50K), 18 (50/500K), and 24 (5/500K) individual single-channel current-voltage (*I/V*) relationships, obtained by linear change of the membrane voltage from +140 to −140 mV in 30 msec ramps. The original records were filtered at 2 kHz and sampled at 5 kHz. For comparison, the extrapolations of *I/V* relationships, obtained in symmetrical 5, 50, and 500 mM KCl (data of Fig. 2*b*), by 4th order polynomials are drawn (solid lines). The voltage and current convention is as follows: the voltage is the difference of cytosol minus vacuole, and positive current reflects efflux of cations from the cytosolic side into the vacuole.

which control the conduction of these ions in the SV channel pore. Single channel *I/V* relationships have been analyzed in symmetrical solutions of NaCl (Fig. 2*a*) or KCl (Fig. 2*b*) in the range of concentrations of 5 to 500 mM. To reduce the inhibition of single-channel current by Ca^{2+}, the free Ca^{2+} concentration was lowered to 50 μM, which was still sufficient to promote a stable SV channel activity at all conditions. At low (5 mM) concentration of KCl or NaCl, however, we required large (110–140 mV) positive potentials to activate the channel. This might be due to low Cl^- concentration, as cytosolic Cl^- is a positive regulator of the SV channel activity (Pantoja, Dainty & Blumwald, 1992*a*). The single channel *I/V* relationships deviated from linear behavior at all conditions. It was especially evident at low Na^+ or K^+ concentration (Fig. 2*c*), when inward rectification of the single-channel current was prominent. The preferential suppression of the outward current was gradually relieved with the increase of cation concentration, and at concentrations of $Na^+ \geq 100$ mM or $K^+ \geq 300$ mM, the *I/V* curves at positive potentials displayed an ascending, exponential-like trend. At all concentrations the single-channel current tended to saturate at high positive potentials, with the saturation level increasing with the increase of concentration of the permeant cation. For the purpose of the present study we needed to evaluate the single-channel conductance at zero voltage (which here is equal to the chord conductance as the ionic current in symmetrical conditions always reversed at zero voltage) as a function of cation concentration (activity). To do this, we have formally described the *I/V* curves by low order polynomials. The 4th order polynomial already fairly explained the curve shape (*result not shown*). Then we took the coefficient of the linear (1st order) term, which defines the value of the first derivative (conductance) at zero potential, and plotted it as a function of cation activity (Fig. 3). The resulting dependence for K^+ could be explained by simple Michaelis-Menten type binding isotherm (Fig. 3*b*), with a maximal conductance of 385 ± 27 pS and K_m of 103 ± 14 mM. Alternatively, we have fitted the data by Eq. 2, yielding 334 ± 25 pS, 152 ± 37 mM, and 1.18 ± 0.09 for maximal conductance, K_m, and Hill coefficient, respectively. Although this approach resulted in a visually better description of experimental points, the F-test indicated that the two approaches describe the data equally with a probability of 0.74. Fitting the data points of the Na^+ series to the Michaelis-Menten equation (Eq. 1) yielded a maximal conductance and K_m of 301 ± 21 pS and 64 ± 9.5 mM, respectively. However, based on a statistical comparison of fits given by Eq. 1 and by Eq. 2 with the experiment, the data points could be better described by cooperative binding (Eq. 2), with maximal conductance of 263 ± 12 pS, K_m of 20 ± 7.4 mM, and Hill coefficient $n = 1.25 \pm 0.08$ (Fig. 3*a*), than by Eq. 1 (F-test 0.05).

Characterization of the Unitary Currents Carried by Magnesium and Calcium

To insure that the currents observed in isolated patches are mediated by a unique type of channel, the SV channel, we routinely tested their activation kinetics by application of steps from negative to positive membrane voltages. A typical example of such recording in symmetrical 0.5 mM Ca^{2+} and in symmetrical 0.5 mM Mg^{2+} solutions, respectively, is presented in Fig. 4. Steps to negative potentials (−20 to −100 mV) did not evoke any single-channel currents. In case of 0.5 mM Mg^{2+}, the delayed activation of single-channel currents was observed starting at +40 mV, and the steady state activity reached its maximum at potentials >+120 mV (Fig. 4). It should be noted that magnesium by itself failed to activate the SV channel (*data not shown*). Therefore, in this experiment and in all experiments for Mg^{2+} concentrations between 0.5 and 30 mM, the bath and pipette solutions were supplemented with Ca^{2+} at a free concentration of 50 μM (20 μM in the case of 0.2 mM Mg^{2+} solution). In case of symmetrical 0.5 mM Ca^{2+}, the SV channels required much higher potentials (>+100 mV) and longer times (note different time scales in Fig. 4) for their activation. It is known that the activation kinetics

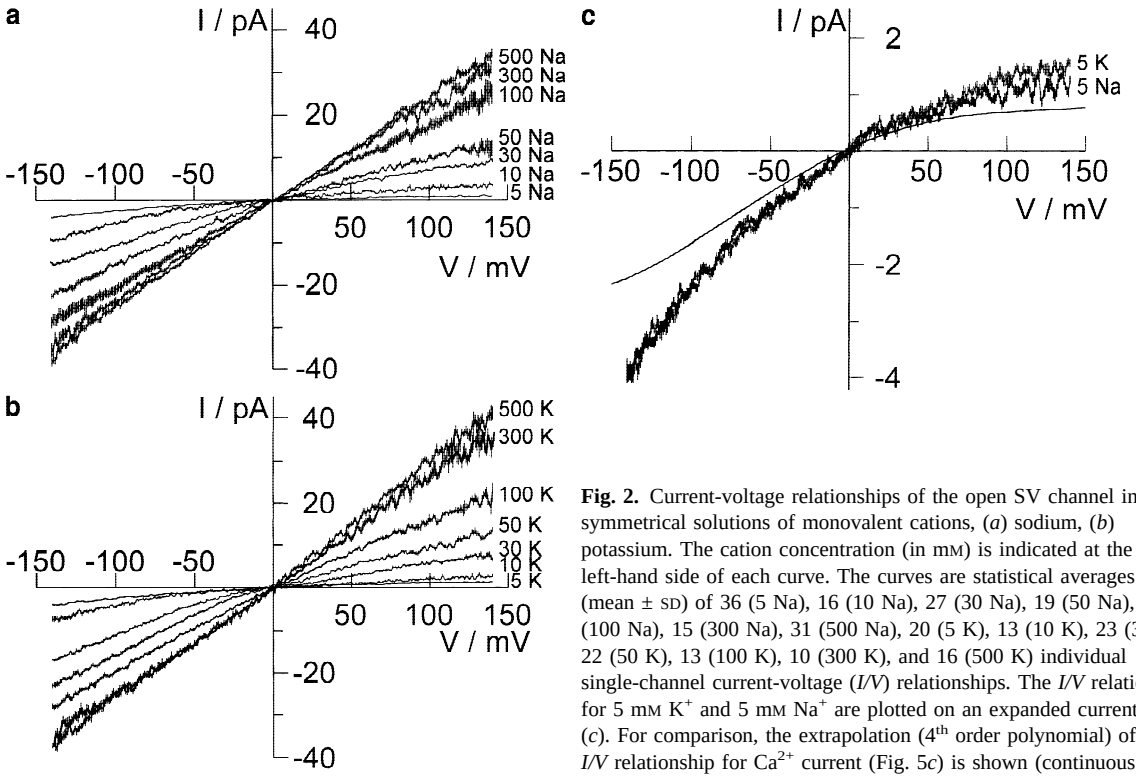

Fig. 2. Current-voltage relationships of the open SV channel in symmetrical solutions of monovalent cations, (*a*) sodium, (*b*) potassium. The cation concentration (in mM) is indicated at the left-hand side of each curve. The curves are statistical averages (mean ± SD) of 36 (5 Na), 16 (10 Na), 27 (30 Na), 19 (50 Na), 24 (100 Na), 15 (300 Na), 31 (500 Na), 20 (5 K), 13 (10 K), 23 (30 K), 22 (50 K), 13 (100 K), 10 (300 K), and 16 (500 K) individual single-channel current-voltage (*I/V*) relationships. The *I/V* relations for 5 mM K^+ and 5 mM Na^+ are plotted on an expanded current scale (*c*). For comparison, the extrapolation (4^{th} order polynomial) of the *I/V* relationship for Ca^{2+} current (Fig. 5*c*) is shown (continuous line).

of the SV current are a function of luminal Ca^{2+}, being the slower the higher the Ca^{2+} concentration in the vacuole, whereas the effect of vacuolar Mg^{2+} could be compared with one produced by 100-times lower Ca^{2+} concentration (Pottosin et al., 1997, 2000). Therefore, the difference in activation kinetics between two patches, observed in Fig. 4, was to be expected and reflected a 10-fold increase of vacuolar Ca^{2+}, from 0.05 mM to 0.5 mM. However, a large shift of threshold potential in the presence of Mg^{2+} needs to be explained. According to our data (Pottosin et al., 1997, 2000), the effects of an equivalent increase of cytosolic and vacuolar Ca^{2+} on the channel voltage dependence cancelled each other, and in this case cytosolic/vacuolar free Ca^{2+} concentration was symmetric, 0.05/0.05 mM and 0.5/0.5 mM, respectively. Experiments, presented in Fig. 4, were performed on the same vacuolar preparation, displaying a highly reproducible level of the voltage-dependent SV channel activity at equivalent ionic conditions. Apparently, the difference in voltage threshold could be attributed to the presence of 0.5 mM Mg^{2+} at the cytosolic face of the patch, because vacuolar Mg^{2+}, in contrast to vacuolar Ca^{2+}, at this concentration hardly affected the SV channel activity. This conclusion confirmed the recent finding by Pei and coworkers (1999) on guard cell vacuolar preparation, that millimolar cytosolic Mg^{2+}, being incapable to activate the SV channel by itself, strongly promoted the activation of the channel by cytosolic Ca^{2+}.

In the presence of Ca^{2+} as unique charge carrier the SV channel displayed a quick rundown of activity. In the inset of Fig. 4 the steady-state activity of the SV channel at +200 mV is presented, observed 15 minutes after the first recording taken 2–3 minutes after patch isolation. The rundown was typical for all patches examined in concentrations of 0.2–1 mM Ca^{2+}; therefore, we needed to accumulate a large number of successful patches (up to 7) for each Ca^{2+} concentration in order to obtain sufficient averages of single-channel *I/V* relationships. In contrast, in the presence of Mg^{2+}, the rundown was much slower, and we could still register a substantial SV channel activity up to 1–2 hr after patch isolation. Thus, we restricted ourselves to 2 successful patches for each Mg^{2+} concentration.

Current-voltage relationships of the open SV channel have been analyzed in the 0.2–30 mM range of divalent cation concentrations. Selected *I/V* relationships, obtained in symmetrical solutions of 10, 1.0, and 0.2 mM Mg^{2+} or Ca^{2+} are presented in Fig. 5*a,b*. The currents saturated already at 1 mM concentration, so no significant difference was observed between *I/V* curves obtained at 1 mM and 10 mM of divalent cation. Curves for 3 mM and 30 mM concentrations (*not shown* for clarity) perfectly fitted those obtained with 1 and 10 mM. At saturating concentrations, e.g., at 10 mM, a marked difference was observed in the magnitude of currents, carried by Ca^{2+} and Mg^{2+}, and in the shape of corresponding *I/V* relations (Fig. 5*c*). Whereas with Mg^{2+}, an N-shaped curve was observed, with an exponential-like increase of

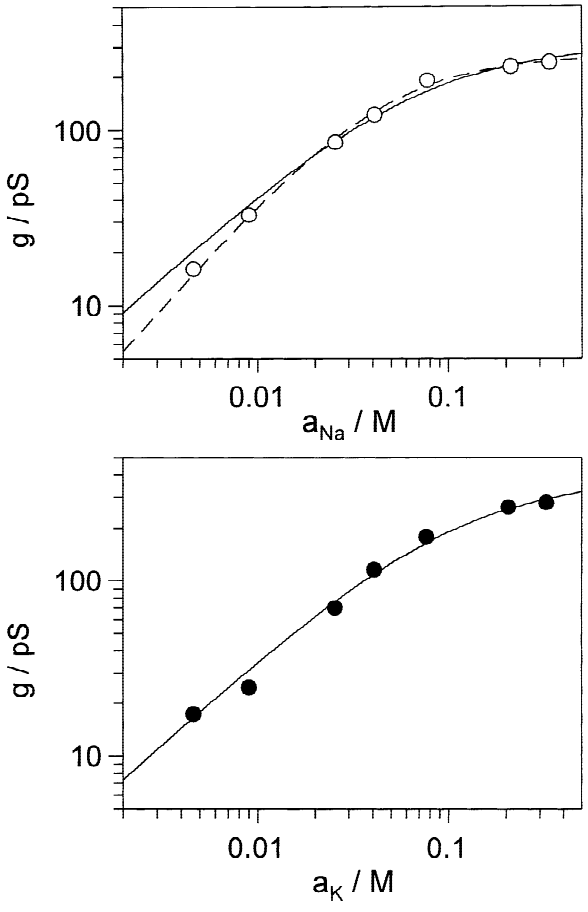

Fig. 3. Conductance-activity relations of the monovalent cation current through the open SV channel at zero voltage. The concentrations of sodium (upper plot) and potassium (lower plot) were converted to ionic activities, a_{Na} and a_K, in mole/liter (M). The data points are the coefficients of the 1st order term of the fits of current-voltage relations, presented in Fig. 2, to 4th order polynomials. The solid lines are best fits to the Michaelis-Menten equation (Eq. 1) with maximal conductance 301 ± 21 pS and 385 ± 27 pS, and K_m of 64 ± 9.5 mM and 103 ± 14 mM for Na^+ and K^+, respectively. Alternatively, the data for Na^+ were fitted to Eq. 2 (dashed line), yielding maximal conductance of 263 ± 12 pS, K_m of 20 ± 7.4 mM, and Hill coefficient $n = 1.25 \pm 0.08$.

current at large positive and negative potentials, with Ca^{2+} as unique charge carrier, the *I/V* curve displayed marked inward rectification, with a sharp saturation of single-channel current at potentials >+50 mV. In one experiment, by combining the maximum of holding- and command potentials provided by the amplifier (200 mV + 200 mV = 400 mV), we were able to perform a stable recording of the SV channel currents at +400 mV with Ca^{2+} (1 mM) as unique charge carrier. A representative trace is given in Fig. 5*d*. It can be seen that the amplitude of the single-channel current at +400 mV was not different from that obtained at +100 to +140 mV in a routine experiment (Fig. 5*b*) or at +200 mV (Fig. 4, *inset*). The saturation level (~0.7 pA) of the single-channel current at positive potentials was apparently independent on Ca^{2+} concentration in the range of 1–30 mM (Fig. 5*b* and 6*b*).

The unitary current started to decrease at 0.5 mM Mg^{2+} or Ca^{2+}, and at a concentration of 0.2 mM the decrease could be seen clearly. Regretfully, we could not perform measurements with lower Ca^{2+} concentrations, as the activity of the channel almost disappeared. Already with 0.5 mM Ca^{2+}, as mentioned above, we needed to set the activation voltage to +200 mV, and even at these conditions the activity was seldom (Fig. 4, *inset*). And with 0.2 mM symmetrical Ca^{2+} the situation was even worse, so that in only less than half of the patches we could make successful recordings. With 0.2 mM Mg^{2+} supplemented with 20 μM Ca^{2+} we still observed a stable single-channel activity at potentials around +150 mV, but we encountered problems with further lowering of Mg^{2+} concentration. We intended to keep a Mg^{2+}/Ca^{2+} ratio of at least 10 to diminish interference between the two different cations, however, lower concentration of cytosolic Ca^{2+} and, possibly, also of Cl^- (Pantoja et al., 1992*a*) resulted in vanishing small activity of the SV channels. Nevertheless, a relatively small scattering of single-channel data allowed us to extrapolate binding isotherms for the chord conductance (Fig. 6*a*) and for the single-channel current at +100 mV (Fig. 6*b*) to concentrations below the experimental range. The curves could be fairly explained by simple Michaelis-Menten (Eq. 1) binding isotherms, with maximal conductance for Mg^{2+} and Ca^{2+} of 18.0 ± 0.4 pS and 13.0 ± 0.3 pS, and values for K_m of 0.038 ± 0.011 mM and 0.080 ± 0.018 mM, respectively (Fig. 6*a*). Similar fitting of the single-channel currents at +100 mV yielded maximal current of 1.62 ± 0.03 and 0.77 ± 0.03 pA, and K_m of 0.093 ± 0.013 and 0.165 ± 0.032 mM for Mg^{2+} and Ca^{2+}, respectively (Fig. 6*b*). The voltage-dependence of the apparent dissociation constant was similar to that observed for monovalent cations (Fig. 2) where single-channel currents at negative potentials saturated at lower concentrations of permeant cation as compared to currents at positive potentials. An alternative fit of the data to Eq. 2 (*not shown*) yielded Hill coefficients, *n*, for the chord conductance of 1.04 ± 0.20 and 1.01 ± 0.06, and for the current at +100 mV of 0.97 ± 0.29 and 1.25 ± 0.12, for Mg^{2+} and Ca^{2+}, respectively. Only in the last case, for the current at +100 mV carried by Ca^{2+}, Eq. 2 explained the data somewhat better than Eq. 1, albeit the difference was statistically insignificant (F-test 0.80). The experiments presented in Figs. 5 & 6 clearly indicate the presence of saturable high-affinity binding site(s) for divalent cations within the SV channel pore. It should be noted here, that, although most of our data formally could be explained by a simple binding mechanism, it does neither imply existence of the unique binding site nor single-ion occupancy of the pore. Simultaneous

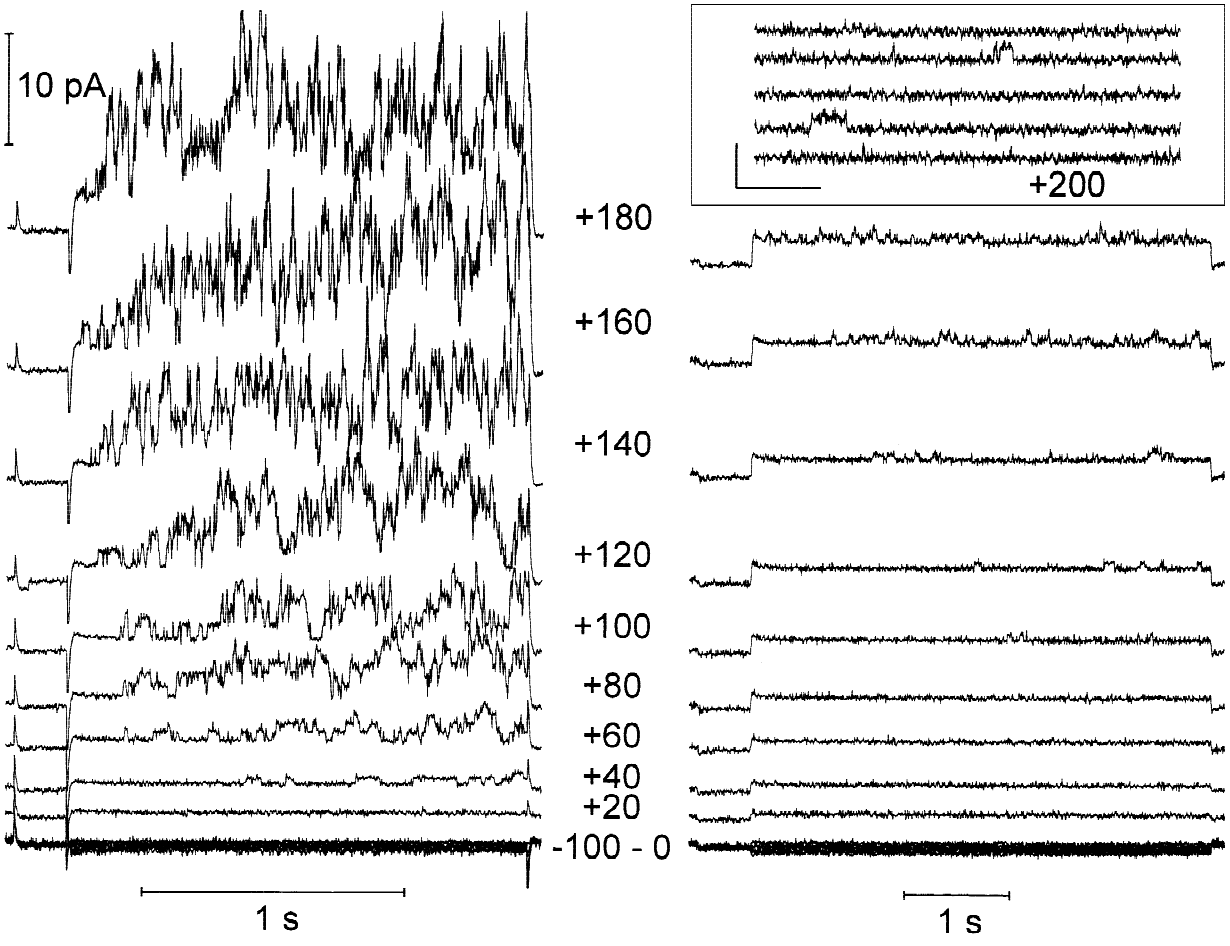

Fig. 4. Example of voltage- and time-dependent activation of single-channel currents carried by magnesium and calcium. Single-channel currents were recorded on small vacuolar-side-out patches isolated from the vacuoles of the same preparation. The patches were bathed in symmetrical 0.5 mM Mg^{2+} + 0.05 mM Ca^{2+} (left) or 0.5 mM Ca^{2+} (right); *see* Materials and Methods for the detailed composition of experimental solutions. The voltage was stepped from a holding level of −40 mV to potentials from −100 mV to +180 mV as indicated. The duration of the step was 1.76 sec and 4.4 sec, and sampling rate was 0.5 kHz and 0.2 kHz for Mg^{2+} and Ca^{2+}, respectively (note different time scales). No leak subtraction was done, and the seal resistance for both patches was ~110 GΩ. Inset shows a steady-state record of single-channel currents carried by Ca^{2+} at +200 mV (sampled at 2 kHz and filtered at 1 kHz, calibration bar 2 pA and 0.1 sec, respectively) for the same experiment as presented below, but taken at 15 min rather than 2–3 min after the patch isolation.

binding of several ions with a similar affinity to weakly interacting sites may produce the same behavior.

Discussion

Conductance and Selectivity of the Slow Vacuolar Channel

This study, to our knowledge, is the first systematic report describing the conductance-activity relations for physiologically important cations, Na^+, K^+, Ca^{2+} and Mg^{2+}, in the SV channel. The key findings of this work may be summarized as follows: the channel pore contains saturable binding sites, high-affinity for divalent cations and low-affinity for monovalent ones. As a virtue of this fact, the divalent cations reside longer time within the pore and conducted more slowly compared to the monovalent ones. However, the Mg^{2+} and Ca^{2+} conductance is substantial and approaches maximal level, 18 and 13 pS, respectively, already at physiological concentrations of these ions (Fig. 6*a*).

The competition of divalent and monovalent cations for the conduction pathway may partly explain a diversity of single-channel conductance values reported in the literature for the SV channels (see Schulz-Lessdorf & Hedrich, 1995 for a review). As an example, for the SV channel from red beet vacuoles a 70 pS single-channel conductance for symmetrical 100 mM KCl was reported previously (Schulz-Lessdorf & Hedrich, 1995; Gambale

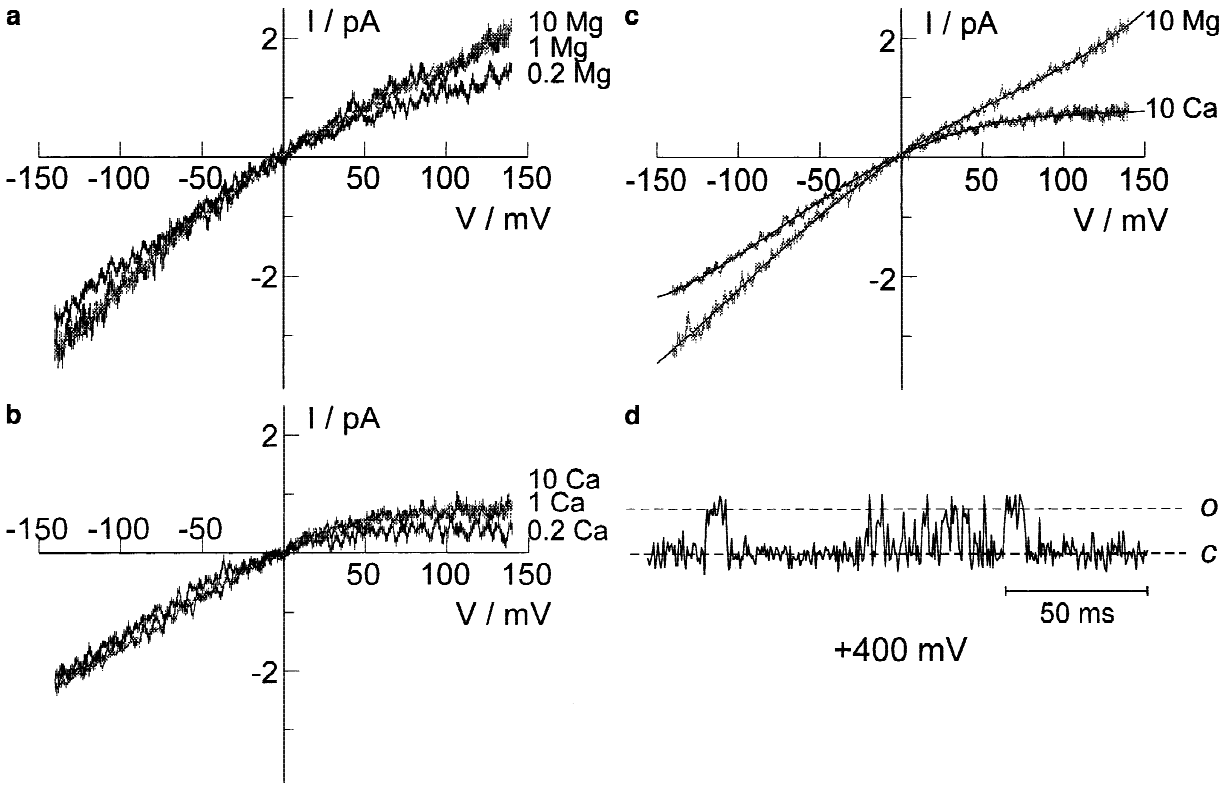

Fig. 5. Current-voltage relationships of the open SV channel in symmetrical solutions of divalent cations, (*a*) magnesium, (*b*) calcium. The divalent concentration (in mM) is indicated at the left-hand side of each curve. The curves are statistic averages (mean ± SD) of 73 (0.2 Mg), 26 (1 Mg), 32 (10 Mg), 43 (0.2 Ca), 28 (1 Ca), and 58 (10 Ca) individual single-channel current-voltage (*I/V*) relationships. The number of patches used for each concentration point was 2 for Mg-series, and 4, 7, and 7 for 10, 1, and 0.2 mM Ca^{2+}. For better resolution the curves for 10 mM Mg^{2+} or Ca^{2+} are shown in gray. These curves are re-plotted (*c*) and 4th order polynomials, fitted to the data, are shown (continuous lines). The saturation of the single-channel current carried by Ca^{2+} at cytosol-positive potentials is confirmed by unique recording in symmetrical 1 mM Ca^{2+} solution at +400 mV. This clamping-voltage was achieved by simultaneous application of the maxima of holding (+200 mV) and of command (+200 mV) voltages provided by the patch-clamp amplifier. A representative burst of single-channel activity from this record, filtered at 1 kHz and sampled at 2 kHz, is shown in (*d*). The calibration of the amplitude of the record was the same as that of the current axis in (*b*) to facilitate the comparison; *c* and *o* indicate closed and open channel levels, respectively.

et al., 1996) compared to 179 pS for the same concentration (Fig. 3*b*, this study). The only difference between ionic conditions of this and previous studies was the inclusion of 0.05 mM Ca^{2+} or 1 mM Ca^{2+} plus 2–5 mM Mg^{2+}, respectively; so, obviously, the high concentration of divalent cations caused more than a two-fold inhibition of single-channel current, mainly carried by K^+ under these conditions. The competition of divalent cations with K^+ hardly affected the maximal conductance for K^+, observed at saturating concentrations of this ion, but shifted the conductance-activity relation to higher K^+ concentrations. The apparent K_m for K^+ changed from ~100 mM at low Ca^{2+} (this study) to ~250 mM at millimolar concentrations of divalent cations (Gambale et al., 1996). The competition between divalent and monovalent cations for the pore appears to be dependent not only on absolute concentrations, but also on the concentration ratio. Particularly, the shape of current-voltage relationships at low Na^+ or K^+ concentration (and low Na^+, K^+/Ca^{2+} ratio, ~100) almost repeats the shape of current-voltage relationships observed in pure Ca^{2+} solutions as if the passage of Ca^{2+} ion modulates the overall ion flux across the channel under these conditions (Fig. 2*c*). And increase of monovalent to divalent cation ratio by ~10 times caused a transformation from inwardly rectifying to an almost symmetrical current-voltage relation (Fig. 2*a*,*b*).

The competition between divalent and monovalent cations for the entrance into the pore also affected reversal potential measurements under asymmetrical ionic conditions. In this study we have revealed that when monovalent cation to Ca^{2+} ratio was 1000 or 10000 at both membrane sides (500/50 mM KCl gradients), the observed reversal potential almost ideally fitted the Nernst potential for K^+ ion, formally implying 1% Cl^-/K^+ relative permeability at the most. However, when the concentration of K^+ at one membrane side was lowered from 50 to 5 mM (K^+/Ca^{2+} ratio ~100), the reversal po-

tential deviated by 25–30 mV from the equilibrium potential for K^+ (Fig. 1). Obviously, the evaluation of Cl^- to K^+ relative permeability on the basis of reversal potential measurements in the first case comes closer to the reality. Use of higher (millimolar) Ca^{2+} concentrations and, consequently, less favorable K^+/Ca^{2+} ratios resulted in a further overestimation of Cl^- to K^+ relative permeability, from 5–10% (Ward & Schroeder, 1994; Allen & Sanders, 1995) up to 30% (Schulz-Lessdorf & Hedrich, 1995), depending on particular ion conditions and calculation approaches. It is for the first time experimentally shown in the present study, that the true Cl^-/K^+ permeability ratio is below 1%, thus leaving virtually no room for anion flux through the SV channel.

Organization of the SV Channel Conduction Pathway

A novel finding of this work was a high unitary conductance of the SV channel for Mg^{2+} ion. Magnesium has a very special position among physiologically abundant cations due to its strong degree of hydration. Unlike, for instance, Ca^{2+}, which exchanges water molecules in its inner hydration shell in the nanosecond time scale, Mg^{2+} requires 10^{-5} sec for water replacement (Hille, 1992). Simple calculation shows that if Mg^{2+} needs to lose a single water molecule to pass the selectivity filter of the channel, this step becomes already rate-limited in the overall conduction, and resulting current will not exceed 40 fA. Consequently, voltage-dependent Ca^{2+} channels do not display any measurable Mg^{2+} conduction (Hille, 1992). If Mg^{2+}, as in this work (Figs. 4, 5), carries a current in the pA-range, this unequivocally implies that this cation preserves the inner shell of waters all the way through the channel pore. This could be possible only if the minimal diameter of the channel pore is $\geq$7 Å. This agrees with our previous estimate of the pore caliber using a variety of organic blockers of different size (Dobrovinskaya et al., 1999). The large cut-off value is at the upper limit still allowing selective permeability for inorganic ions (Hille, 1992).

The unitary current carried by divalent cations, Mg^{2+} and Ca^{2+}, at concentration as low as 0.2 mM at negative potentials did not show saturation until −2.5 pA level (Fig. 5). The diffusion-limited current (I_{lim}) could be evaluated using the approach described by Hille (1992):

$$I_{lim} = 2\,\pi \cdot a \cdot D \cdot c \cdot z \cdot F \qquad (3)$$

where a is the radius of the pore entrance (in cm), D is a diffusion coefficient, 0.75×10^{-5} cm^2/sec for Ca^{2+} or Mg^{2+}, the ionic concentration is $c = 2 \times 10^{-7}$ mole/cm^3, the valence, $z = 2$, and F is Faraday's constant, 9.65×10^4 C/mole. The evaluation of an unknown radius of the

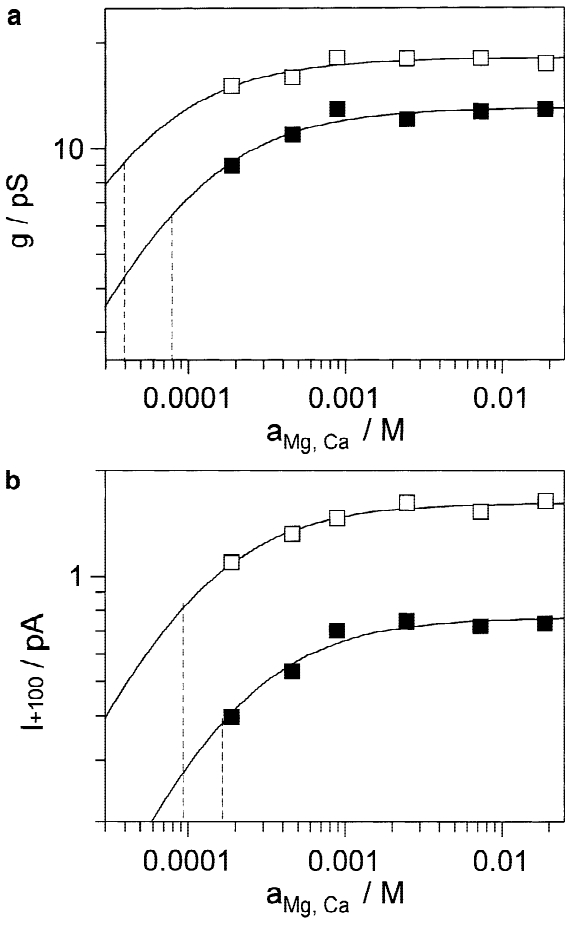

Fig. 6. Conductance- and current-activity relations for the divalent cations in the open SV channel. (*a*) Single-channel conductance at zero voltage as a function of Mg^{2+} (□) or Ca^{2+} (■) activity. The data points are the coefficients of the 1st order term of the fits of current-voltage relations, as those presented in Fig. 2, to 4th order polynomials. Additional data points for symmetrical 0.5 mM, 3 mM and 30 mM of Mg^{2+} or Ca^{2+} with a comparable number of averages were included. Continuous lines are best fits to the Michaelis-Menten equation with a maximal conductance of 18.0 ± 0.4 and 13.0 ± 0.3 pS, and K_m of 0.038 ± 0.011 and 0.080 ± 0.018 mM for Mg^{2+} and Ca^{2+}, respectively. (*b*) Single-channel currents carried by Mg^{2+} (□) or Ca^{2+} (■) at +100 mV as a function of divalent cation activity. The SD for mean current values were <0.1 pA. Solid lines are best fits to the Michaelis-Menten equation with maximal current of 1.62 ± 0.03 and 0.77 ± 0.03 pA, and K_m of 0.093 ± 0.013 and 0.165 ± 0.032 mM for Mg^{2+} and Ca^{2+}, respectively. Dashed lines connected to corresponding curves indicate the approximate values of dissociation constants (K_m).

SV channel pore entrance to produce 2.5×10^{-12} A current yields a value of 1.4×10^{-6} cm or 140 Å! For a more realistic value of 10 Å one needs a 14-fold increase of the local concentration of the divalent cation, which could be achieved only by fixed negative charge in the proximity of the vacuolar pore entrance. The same is true for the cytosolic pore mouth, based on the magnitude of currents at positive potentials. We came to a similar assumption

based on the absolute rates of ruthenium red collision with the cytosolic mouth of the SV channel as a function of the bulk concentration of the substance (Pottosin, Dobrovinskaya & Muñiz, 1999). Existence of fixed negative charges in the vestibules of the channel pore seems to be a general feature of cation channels of animal and plant cells (Hille, 1992; White, 2000). This structural feature serves to concentrate the cations and to promote their fluxes at low concentration. On the other hand, it builds an additional barrier on the way of anions, contributing to the high cation over anion selectivity of the channel.

Recently the rate theory was applied to describe K^+ and Ca^{2+} conduction in the SV channel by single-site binding models (Allen et al., 1998). Although such models apparently ignored the multi-ion nature of the SV channel (Allen & Sanders, 1996; Gambale et al., 1996; Dobrovinskaya et al., 1999), they might serve as initial clue, offering a number of testable predictions. Particularly, conduction of Ca^{2+} in the SV channel provided a peculiar pattern, with a sharp saturation of single-channel current at positive voltages which could be traced up to +400 mV (Fig. 5*b*,*d*), and which was independent of the concentration of Ca^{2+} in the range of 1 to 30 mM (Fig. 6*b*). On theoretical grounds, a conventional two-barrier-one-well (2B-1W) model, with fixed positions of binding site (well) and barriers could not explain such a behavior. As an alternative, a "dynamic-pore" version of 2B-1W model (Allen et al., 1998), assuming a carrier-like fluctuation of the potential profile within the pore, might be applied. To describe the saturation of single-channel current carried by Ca^{2+} (Fig. 5*b*) one needs to postulate that this conformational transition is voltage-independent and becomes rate-limiting at high positive potentials. The "dynamic-pore" is, therefore, the only possible alternative among single-site models, which could in principle explain our data. However, it is more likely in the context of previous findings, that multi-well (and multi-ion) models are better suited to describe the conduction within the SV channel pore.

Comparison with Other Ca^{2+}-Permeable Channels

We are aware of just one previous report, analyzing the unitary currents of a Ca^{2+}-permeable channel at micromolar Ca^{2+} activity, the work of Piñeros and Tester (1997) on the *rca* channel from wheat root plasma membrane incorporated into planar lipid bilayer. The *rca* channel displayed a Ca^{2+} binding affinity very similar to that of the SV channel, 99 and 80 μM, respectively. Another channel, which has a similar (predicted) K_m for Ca^{2+} and Mg^{2+} of 116 and 86 μM, respectively, is the ryanodine receptor (RyR) channel of cardiac muscle sarcoplasmic reticulum (Tinker, Lindsay & Williams, 1992). Interestingly, all three aforementioned channels, including the SV channel, are specifically sensitive to ruthenium red (Ma, 1993; Piñeros & Tester, 1997; Pottosin et al., 1999). All three channels mentioned above have a moderate selectivity for divalent over monovalent cations, which does not exceed a factor of 7 for the SV and RyR channel (Pantoja et al., 1992*b;* Tinker et al., 1992; Ward & Schroeder, 1994) and is slightly higher, $P_{Ca^{2+}}/P_{K^+}$ ranging from 17 to 41, in the *rca* channel (Piñeros & Tester, 1997). These characteristics clearly discern these three Ca^{2+}-permeable channels from voltage-dependent Ca^{2+} channels of animal cell plasma membrane. The latter are characterized by high ($\sim 10^3$) divalent over monovalent cation selectivity, large values of K_m (5–28 mM) for the divalent cation conductance, and do not conduct Mg^{2+} (Kostyuk, Mironov & Shuba, 1983; Hess, Lansman, & Tsien, 1986; Hille, 1992).

Availability of detailed characteristics of the SV channel current for a broad range of voltage and cation concentrations provided us with a diagnostic tool to challenge the variety of Ca^{2+} pathways reported for the vacuolar membrane of higher plants. To our surprise, the conductance properties of the SV channel reported here were quantitatively identical to the characteristics of the so-called voltage-dependent vacuolar Ca^{2+} channel (VVCa) from the same preparation (Johannes & Sanders, 1995; Allen & Sanders, 1997). This included equal conductance for Mg^{2+}, Ca^{2+}, Ba^{2+}, and for K^+ (Pantoja et al., 1992*b;* Johannes & Sanders, 1995; this work) and K_m values for Ca^{2+} and K^+, directly measured in this work for the SV channel and theoretically approximated for the VVCa (Allen et al., 1998). However, the SV channel is activated by cytosol positive membrane voltage and by cytosolic Ca^{2+} (Hedrich et al., 1988), while the VVCa was reported to be gated open by negative voltage and by increase of vacuolar Ca^{2+} (Johannes & Sanders, 1995). Besides the opposite "sidedness" of the effects, however, the voltage and Ca^{2+} sensitivity of both channels was fairly similar as if the characteristics of the VVCa channel formed a mirror image of those of the SV channel (cf Johannes & Sanders, 1995 and Pottosin et al., 1997, 2000). The simplest explanation of this peculiarity is that reported characteristics of the VVCa channel are a manifestation of the same SV channel, but measured on inverted patches. A convincing argument against this hypothesis may be the recording of whole vacuole currents with all characteristics (kinetics, Ca^{2+} and voltage-dependence, rectification of instantaneous current under bi-ionic conditions) pertinent to those reported for single VVCa channels. Due to the lack of such coherent evidence, identification of the additional voltage-dependent Ca^{2+}-permeable channel in the vacuolar membrane, the VVCa channel, might require further experimental proof.

The authors wish to thank Mrs. Ondina Popescu for her qualified technical assistance in some experiments. This work was supported by

research grant 29473N of the Consejo Nacional de Ciencia y Tecnologia (CONACyT) to I.I.P.

References

Allen, G.J., Sanders, D. 1995. Calcineurin, a type 2B protein phosphatase, modulates the Ca^{2+}-permeable slow vacuolar ion channel of stomatal guard cells. *Plant Cell.* **7:**1473–1483

Allen, G.J., Sanders, D. 1996. Control of ionic currents in guard cell vacuoles by cytosolic and luminal calcium. *Plant J.* **10:**1055–1069

Allen, G.J., Sanders, D. 1997. Vacuolar ion channels of higher plants. *Adv. Botanical Res.* **25:**217–252

Allen, G.J., Sanders, D., Gradmann, D. 1998. Calcium-potassium selectivity: Kinetic analysis of current-voltage relationships of the open, slowly activating channel in the vacuolar membrane of *Vicia faba* guard-cells. *Planta* **204:**528–541

Ammann, D. 1986. Ion-Selective Microelectrodes. Springer-Verlag, New York

Amodeo, G., Escobar, A., Zeiger, E. 1994. A cationic channel in the guard cell tonoplast of *Allium cepa. Plant Physiol.* **105:**999–1006

Barry, P.H., Lynch, J.W. 1991. Liquid junction potentials and small cell effects in patch-clamp analysis. *J. Membrane Biol.* **121:**101–117

Dobrovinskaya, O.R., Muñiz, J., Pottosin, I.I. 1999. Asymmetric block of the plant vacuolar Ca^{2+}-permeable channel by organic cations. *Eur. Biophys. J.* **28:**552–563

Gambale, F., Bregante, M., Stragapede, F., Cantu, A.M. 1996. Ionic channels of the sugar beet tonoplast are regulated by a multi-ion single-file permeation mechanism. *J. Membrane Biol.* **154:**69–79

Johannes, E., Sanders, D. 1995. Lumenal calcium modulates unitary conductance and gating of a plant vacuolar calcium release channel. *J. Membrane Biol.* **146:**211–224

Hamill, O.P., Marty, A., Neher, E., Sakmann, B., Sigworth, F.J. 1981. Improved patch-clamp techniques for high-resolution current recording from cells and cell-free membrane patches. *Pfluegers Arch.* **391:**85–100

Hedrich, R., Barbier-Brygoo, H., Felle, H., Fluegge, U.I., Luettge, U., Maathuis, F.J.M., Marx, S., Prins, H.B.A., Raschke, K., Schnabl, H., Schroeder, J.I., Struve, I., Taiz, L., Zeigler, P. 1988. General mechanisms for solute transport across the tonoplast of plant vacuoles: A patch-clamp survey of ion channels and proton pumps. *Bot. Acta* **101:**7–13

Hedrich, R., Kurkdjian, A. 1988. Characterization of an anion-permeable channel from sugar beet vacuoles: effect of inhibitors. *EMBO J.* **7:**3661–3666

Hess, P., Lansman, J.B., Tsien, R.W. 1986. Calcium channel selectivity for divalent and monovalent cations. Voltage and concentration dependence of single channel current in ventricular heart cells. *J. Gen. Physiol.* **88:**293–319

Hille, B. 1992. Ionic Channels of Excitable membranes, 2nd ed. Sinauer Associates, Sunderland, MA

Kostyuk, P.G., Mironov, S.L., Shuba, Y.M. 1983. Two-ion selecting filters in the calcium channel of the somatic membrane of mollusc neurons. *J. Membrane Biol.* **76:**83–93

Ma, J. 1993. Block by ruthenium red of the ryanodine-activated calcium release channel of skeletal muscle. *J. Gen. Physiol.* **102:**1031–1056

MacRobbie, E.A.C. 1998. Signal transduction and ion channels in guard cells. *Phil. Trans. R. Soc. Lond. B.* **353:**1475–1488

Pantoja, O., Dainty, J., Blumwald, E. 1992*a*. Cytoplasmic chloride regulates cation channels in the vacuolar membrane of plant cells. *J. Membrane Biol.* **125:**219–229

Pantoja, O., Gelli, A., Blumwald, E. 1992*b*. Voltage-dependent calcium channels in plant vacuoles. *Science* **255:**1567–1570

Pei, Zh.-M., Ward, J.M., Schroeder, J.I. 1999. Magnesium sensitizes slow vacuolar channels to physiological cytosolic calcium and inhibits fast vacuolar channels in fava bean guard cell vacuoles. *Plant Physiol.* **121:**977–986

Piñeros, M, Tester, M. 1997. Calcium channels in higher plant cells: selectivity, regulation and pharmacology. *J. Experim. Botany* **48:**551–577

Pottosin, I.I., Tikhonova, L.I., Hedrich, R., Schönknecht, G. 1997. Slowly activating vacuolar channels can not mediate Ca^{2+}-induced Ca^{2+}-release. *Plant J.* **12:**1387–1398

Pottosin, I.I., Dobrovinskaya, O.R., Muñiz, J. 1999. Cooperative block of the plant endomembrane ion channel by ruthenium red. *Biophys. J.* **77:**1973–1979

Pottosin, I.I., Dobrovinskaya, O.R., Muñiz, J. 2000. Ca^{2+}-permeable channel of plant vacuoles sensing Ca^{2+} gradient. *Biophys. J.* **78:**312A

Schulz-Lessdorf, B., Hedrich, R. 1995. Protons and calcium modulate SV-type channels in the vacuolar-lysosomal compartment. Channel interaction with calmodulin inhibitors. *Planta* **197:**655–671

Tinker, A., Lindsay, A.R.G., Williams, A.J. 1992. A model for ionic conduction in the ryanodine receptor channel of sheep cardiac muscle sarcoplasmic reticulum. *J. Gen. Physiol.* **100:**495–517

Ward, J.M., Schroeder, J.M. 1994. Calcium-activated K^+ channels and calcium-induced calcium release by slow vacuolar ion channels in guard cell vacuoles implicated in the control of stomatal closure. *Plant Cell* **6:**669–683

White, P.J. 2000. Calcium channels in higher plants. *Biochim. Biophys. Acta* **1465:**171 189